Satellite formation in drop-on-demand printing of polymer solutions

Stephen Hoath, Graham Martin, Rafael Castrejón-Pita and Ian Hutchings; Institute for Manufacturing, Department of Engineering, University of Cambridge, Mill Lane, Cambridge CB2 1RX, UK

Abstract

High speed photographic images of jets formed from dilute solutions of polystyrene in diethyl phthalate ejected from a piezoelectric drop-on-demand inkjet head have been analyzed in order to study the formation and distribution of drops as the ligament collapses. Particular attention has been paid to satellite drops, and their relative separation and sizes. The effect of polymer concentration was investigated.

The distribution of nearest-neighbour centre spacing between the drops formed from the ligament is better described by a 2-parameter modified gamma distribution than by a Gaussian distribution.

There are (at least) two different populations of satellite size relative to the main drop size formed at normal jetting velocities, with ratios of about three between the diameters of the main drop and the successive satellite sizes. The distribution of the differences in drop size between neighbouring drops is close to Gaussian, with a small non-zero mean for low polymer concentrations, which is associated with the conical shape of the ligament prior to its collapse and the formation of satellites.

Higher polymer concentrations result in slower jets for the same driving impulse, and also a tendency to form ligaments with a near-constant width. Under these conditions the mean of the distribution of differences in nearest-neighbour drop size was zero.

Introduction

High-quality images captured over short timescales with spark light sources have been used recently to study the formation and break-up of ink jets [1, 2]. Others have used lasers for single-shot imaging [3] and stroboscopic illumination to study air entrapment in nozzles caused by ink films [4].

In previous work [1] we demonstrated that the shape of an unbroken inkjet ligament as it extended from the nozzle plane could be accurately represented by a truncated cone aligned from the centre of the orifice towards the head of the inkjet, as shown in Figure 1. By assuming this conical geometry, we were able to estimate the velocities of the satellite drops which form behind the main drop from measurements on single flash images. By an extension of this technique, without relying on the conical shape, we were also able to estimate the average mass flow for the stretching ligament [1].

The present work investigated the effects of incorporating polymer solutes in a simple ink on the sizes and spacing of the satellite drops formed by ligament breakage. There is considerable interest in inkjet fluids containing rather small (typically below 100 ppm (w/w)) concentrations of polymers [5] from the viewpoint of suppressing satellite creation in quite slow (2 m/s) drop-on-demand jets, but in the present work somewhat higher concentrations (from 100 ppm to 1% w/w) of mono-disperse medium molecular weight polystyrene (with MW ≈ 100,000 - 500,000) in diethyl phthalate were used in order to study their effects on satellite formation in faster moving inkjets (typical velocity 6 m/s).

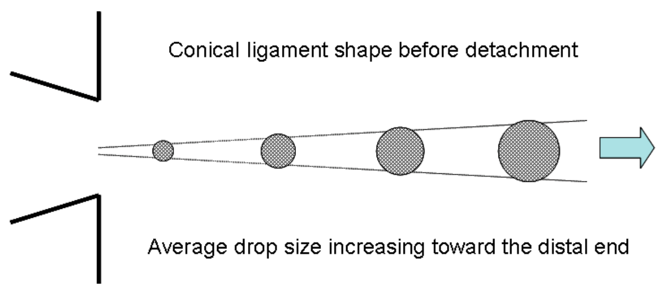

Figure 1: *Schematic representation of the ligament shape near the point of detachment, as found in our previous work on solvent inkjets. The ligament is not cylindrical there but has a form better represented by a truncated cone, with the narrower end at the nozzle and stretching for several hundreds of μm towards the distal end. The lateral width scale is magnified relative to the axial scale.*

Experimental methods and materials

Piezoelectric drop-on-demand (DoD) print heads (Xaar type XJ126-200) were used, in versions with both wetting and non-wetting nozzle plates. The same drive waveform and temperature compensation settings were used for all experiments. The actuation strength settings were controlled through Xaar PCI+ software. For this print head, the actuation strength, which corresponds to the amplitude of the piezo driving voltage, is set via the "EFF" value in the Xaar PCI+ software. Single images were captured using a very short-duration spark light source and a Nikon D70 digital camera with a Navitar x12 zoom lens, as described previously [2]. Precise event timing was achieved (with uncertainty <2 μs) by using a special interface circuit which synchronized the print head firing and clock pulse signals, to allow the triggering of a digital delay unit for the flash illumination at specific line numbers in the printed image. The lines chosen were either the first or the 85th line in the pattern. This synchronization method avoids errors introduced by clock rate changes and software issues, and allows the time delay interval to be preset to within ~100 ns and recorded to within ~10 ns.

Since the object of the study was to observe differences in the distributions of satellite drops formed from the ligament following its detachment from the nozzle, time delays were used which were long enough to allow for the formation of spherical drops; the smaller satellite drops become spherical much more rapidly than the main drop. The distributions of satellite sizes and positions could be studied for different time delays and travel distances from the nozzle plane: for example, at much later times with the print head lifted vertically up out of the field of view.

The DoD actuation waveform was held constant and not optimized for the particular ink properties, and the experiments were performed at a fixed laboratory temperature (21°C). Although the XJ126-200 print head is internally temperature-compensated, the ink temperature is not separately controlled; for the printing conditions used here, the ink temperature was close to the laboratory temperature, which allowed the same temperature compensation algorithm to be used throughout.

Dilute polymer solutions were prepared (by using agitation periods of several weeks to ensure homogeneity) which contained 1-2 wt% of poly-disperse polystyrene (PS: mass weighted molecular weight MW ≈ 196,000) or mono-disperse polystyrene (with various values of MW between 100,000 and 500,000) in diethyl phthalate (DEP) as solvent (with a viscosity of ~ 10 mPas).

These primary solutions were prepared, and their low shear rate (~500 Hz) viscosities determined at 25 ºC, in the Department of Chemical Engineering, University of Cambridge. Further dilutions of these primary solutions were then made with DEP (with final polymer concentrations from 100 ppm to 1 wt%) to give solutions with low shear viscosities between those of pure DEP and the primary solutions (~25 mPa s).

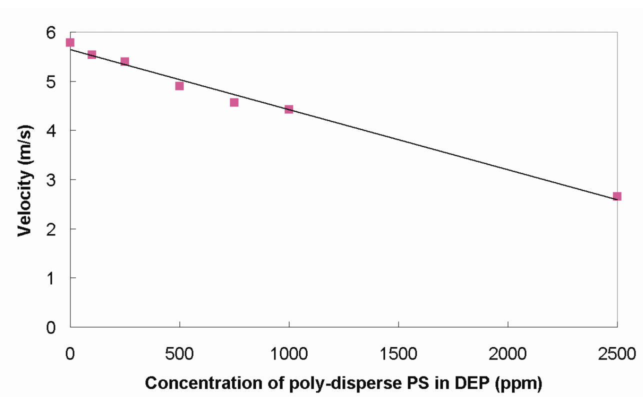

Figure 2: *Effect of concentration of polymer (poly-disperse polystyrene with MW ≈ 196,000)in DEP on jet velocity for a fixed print head actuation setting (chosen to give 6 m/s for the pure solvent).*

The nozzle actuation strength (‘EFF’ value) was adjusted by jetting the pure DEP solvent to give an average speed for the main drops of ~6 m/s, determined by timing their travel between locations 0.8 mm and 1.3 mm from the nozzle plane. The EFF values required to maintain this velocity for the polymer solutions in DEP alone tend to be higher because the solutions have greater viscosity, and because of the other influences of the polymer on the ligament behavior. In some experiments with these solutions the EFF value was maintained at that for the pure solvent, and the main drop velocities were therefore lower than 6 m/s.

Figure 2 shows the influence of the concentration of poly-disperse PS in DEP on the velocity of the main drop, for a fixed EFF value. The velocity fell effectively linearly with increasing concentration, and was halved by the addition of 2500 ppm polymer.

Figure 3 shows a typical image. The nozzle plane lies near the upper edge, as indicated by the arrowed bar which has a length of 1 mm; the images above the bar are reflections in the plane. There are three groups of jets, printed in sequence (a characteristic feature of the Xaar print head design). In the earliest jets, which extend furthest down the image, the ligaments behind the main drops have detached from their nozzles and are in the process of breaking up into satellites. We previously reported that the ligament shapes were effectively conical for long distances behind the heads. As the ligaments break up into drops, there is a tendency for most, if not all, of the satellite drops to move away from the nozzle plane, and such images were used to study how the satellites move relative to the main drop.

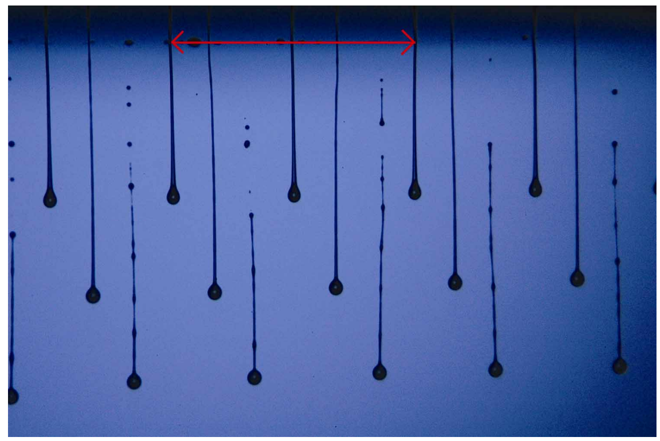

Figure 3: *Jets formed from solutions of polymer in DEP (0.4% mono-disperse polystyrene with MW = 110,000) before and after detachment from the nozzle plane (non-wetting). Such long ligaments and numbers of satellites produced are not examples of optimized printing but of the conditions used to examine the effects of polymer concentration. Residual drops and reflections are visible near the line of nozzles at the top, which is indicated by the position of the double ended arrow of length ~ 1mm.*

Focus conditions were optimized by inspecting the image quality for ligaments and main drops with different positions of the print head, which was mounted on a horizontal X-Y stage. In this way the depth of field (DOF) was determined empirically to be approximately 100 µm at the magnification used in these experiments. This compares reasonably well with a value of 60 µm predicted for a 32 mm working distance from the data sheet supplied by the lens manufacturer.

The pixel shape in the camera CCD is close to square and images of straight edges were used to check for any distortion of the field of view in both horizontal and vertical directions. The linear magnification was determined to be 0.72 µm per pixel from the known separation (137.2 µm) and diameters (50 µm) of the Xaar print head nozzles.

Analysis of some 3D images of jets and drops shows that they are axially symmetrical to better than 2%, unless the jets flex or have tail kinks; these asymmetries can arise from the presence of additives or in jets moving at very low speeds. Full details of the 3D imaging work will be published elsewhere.

The variation of satellite distributions with flight time was also studied by recording images at various delay settings which simultaneously produced measurable satellites for the three nozzle groups (A-B-C), and also by changing the camera mounting to allow portrait-format images and hence observing longer flight times than with landscape-format. This revised mounting also completely eliminated a source of variability in the image position datum which had been compensated for in previous work.

Analysis

Batches of about 50 successive images were recorded with the same delay times relative to the print trigger point and then analyzed with a specially written program, PEJET [1], in order to extract edge profiles. From these processed images, the sizes (i.e. diameters) of the main drops were determined, as well as those of the satellite drops and the separation between neighbouring drops. It was established that the image processing threshold and low size cut-off did not materially affect the profile widths or significantly bias the detection of small drops.

The various distributions were extracted by using an Excel add-in module to filter the image analysis results according to criteria such as drop size, minimum ligament width and satellite location relative to the main axis. The individual batch histograms were inspected before being summed into array averages (covering typically 5 nozzles of each group).

Inspection of the image files also ensured that satellites were not misidentified by the image processing software; those satellites which were too small for automated analysis were logged by hand. All linear dimensions such as drop sizes and drop centre separations are quoted and plotted here in units of pixels, where one pixel represents 0.72 µm. The nozzle diameter of 50 µm is ~69 pixels and in converting drop diameters to volumes it has been assumed that the drops are spherical.

Distributions of drop sizes

A very important difference between the images formed with as single short exposure (as achieved here with a fast, high-brightness flash) and conventional stroboscopic images (based on multiple flashes) lies in the ability to determine satellite sizes and distributions directly from the image.

Figure 4 shows a typical distribution of main drop and satellite sizes (diameters) for jets formed from dilute polymer solutions. The drop sizes are represented as a histogram with bin widths of 1 pixel (0.72 µm) and the data have been summed across part of the print head array visible at this magnification (five nozzles in the same A-B-C group).

The software used to generate this histogram extracts all features wider than a specified threshold; the accuracy of the analysis was also checked by visual inspection of the images. The same method of analysis can be applied to images containing jets, isolated drops and ligaments with incipient drop formation (swellings). The distribution of ligament swellings and satellite sizes is clustered at two widths, labelled large and small, which lie significantly below the main drop size.

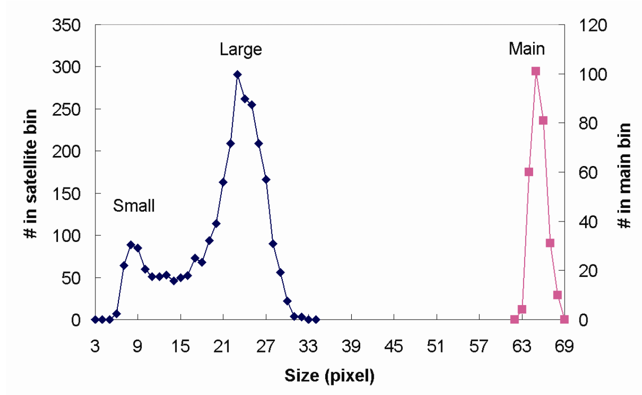

Figure 4: Distribution of main drop and satellite sizes for jets of a dilute solution of polymer (0.1% polystyrene with Mw ≈ 196,000 in DEP) jetted at normal speeds. The data are shown as a histogram with a size bin width of 1 pixel = 0.72 µm. Satellites (and precursor swellings of the ligament) to fall into distinct groups with large and small sizes. There is a definite gap between them and the size of the main drop. The hierarchy of scales is similar to that seen in the ligament width for pendant drops in a viscous fluid [6].

The group labeled 'small' lies above the minimum threshold width of 4 pixels (~3 µm) selected by the drop extraction software, and individual images were inspected to ensure that omission of satellites smaller than this limit had not significantly influenced the conclusions.

Although the existence of still smaller satellite populations might be anticipated [6, 7], with diameters of the order of 1 µm or less, these would not be detectable with the current optical system.

Distributions of drop spacing & size changes

The drop centre spacing values for the image batch can be extracted from the results of the image analysis program, and an example for the same dilute polymer as in Figure 4 is shown here.

The histogram of Figure 5 shows the deduced satellite spacing distribution with a bin width x_0=20 pixels (14.4 µm), without using the average spacing. Such a distribution clearly will have no zero spacing, because the drops have a finite width, but the distribution is also asymmetric, having an extended tail to long separations. Empirical comparisons with possible fitting functions show that a reasonable representation for the shape $f(x$, parameters) of the spacing (x) distribution is given by the 2-parameter modified gamma distribution [8], which may be written $f(x;\alpha,\beta) = x^{(\alpha-1)} e^{-x/\beta} / \beta^{\alpha} \Gamma(\alpha)$, with $\alpha = 3.3$ (i.e. a 2.3 power law in spacing) and a decay length $\beta = 2.2\, x_0$ for a separation length scale of 44 pixels = 32 µm.

Interestingly, it has been reported [9] that the gamma distribution is broadly applicable to the statistics of ligament-mediated spray droplet formation, although in that case the gamma distribution was relevant to the droplet size (rather than separation) resulting from elongation and capillary ligament break-up induced by a rapid airflow over a liquid surface. That example related to the coalescence of the liquid volumes constituting a ligament, whereas in the present case we are studying the detachment and break-up of the ligament.

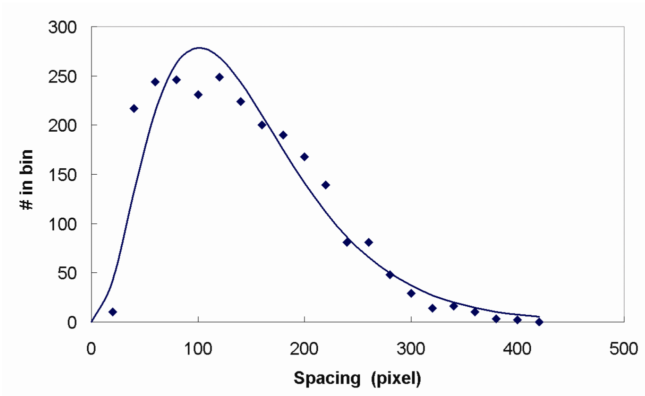

Figure 5: *Distribution of nearest-neighbour drop spacing for jetting of a dilute polymer solution (0.1% poly-disperse polystyrene with MW ≈ 196,000 in DEP), shown as the numbers of satellites found with a given separation, in bins of 20 pixels = 14.4μm width. The solid line superposed on the data is a 2-parameter modified gamma distribution as described in the text.*

Figure 6 shows the corresponding data for the difference in diameter between nearest neighbour satellite drops, which is approximately Gaussian with a mean value of 1.3 pixels = 1.0 μm towards the positive side. This means that on average for this inkjet, more large satellites are found toward the main drop end than at the tail of the ligament.

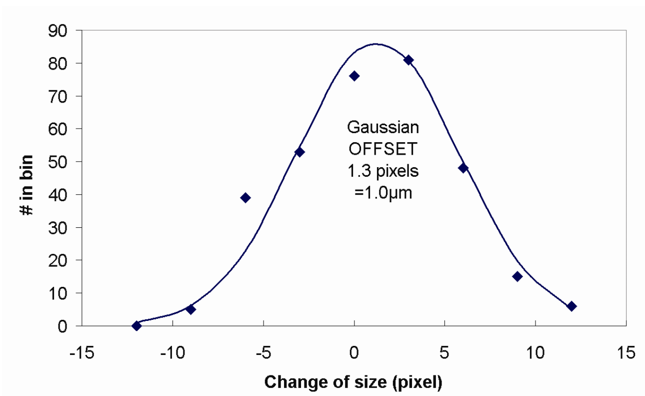

Figure 6: *Distribution of differences in diameter between neighbouring drops for jets formed from a dilute solution of polymer (0.1% polystyrene with MW ≈ 196,000 in DEP) jetted at normal speeds, with a superimposed Gaussian distribution for comparison. The bin size is 3 pixels = 2.2 μm and the mean of the Gaussian is +1.3 pixels = 1.0 μm. This shows that larger satellites form closer to the main drop end of the ligament than towards the nozzle plane of the ligament, which is consistent with the conical shape of the ligament..*

The distribution of the differences in nearest neighbour drop sizes for a jet with a higher polymer content (by a factor of ~4, not shown here) shows no significant correlation between position relative to the inkjet tip and the size of satellites. This may be because the shape of the inkjet ligament for the higher polymer concentration is much closer to cylindrical than in the case of the more dilute solution. However the change in these distributions resulting from different concentrations of the same polymer is very slight.

Discussion

Satellite production appears to be directly related to the strength of the DoD actuation setting used. We have found that both large and small satellites are produced (see Figure 4) as the DoD actuation is increased above a threshold value, since it is possible to produce jets which form only a single main drop and no satellites. As actuation increases, the additional volume of fluid ejected increases the main drop size and also contributes extra satellites; increased actuation increases the production of all satellites, and the additional ligament stretching associated with the increased actuation generates more smaller satellites.

The distribution of nearest-neighbour drop spacings shown in Figure 5 is skewed, with a more gradually decreasing tail towards large spacings rather than a Gaussian decline.

For the very dilute polymer solutions (and the pure DEP solvent), the ligament shape before break-up was a truncated cone. With such a shape, conservation of mass would be expected to favour the formation of larger satellites towards the main drop end if the ligament break-up were to be regular, or to occur at smaller spacings where the ligament is thinner. The bias in the drop size towards the main drop end seen in Figure 6 is therefore not surprising. For the less dilute solutions, the ligament shape before break-up is closer to cylindrical (i.e. the cone has a smaller included angle) and there is much less evidence of a trend in drop size along the ligament.

The variation with flight time of satellite size, difference in size between neighbouring drops and nearest-neighbour spacing can be studied by the methods described here. These aspects are of significant interest because they relate to the influence of the relative velocities and relative sizes of the drops, which result in key events such as the merging of satellite drops with each other or with the main drop. Detailed observations of the effects of flight time will be reported elsewhere; they did not materially affect our conclusions about the satellites and drops formed for the fluids studied in this work.

Conclusions

The application of high speed flash photography, utilizing single high-resolution images, to inkjet phenomena has revealed important underlying aspects of the behaviour of collapsing ligaments and of the resulting droplets. There is evidence for a bias towards the formation of larger satellite drops towards the distal end of ligaments where the ligament before break-up has a pronounced conical shape, as seen for some dilute polymer solutions. This bias is not observed for more cylindrically-shaped ligaments, as seen for example with somewhat higher (but still dilute) concentrations of polymer. Satellite size distributions were found to have at least two distinct peaks, with ratios of about three in linear size (e.g. drop radius or diameter), which are similar to the cascade of length scales found in liquid drops detaching from a free stream under gravity. The distribution of spacings between neighbouring drops exhibits an exponential tail (from a modified gamma distribution), similar to that found for the drop size distribution in ligament-mediated spray formation.

Acknowledgements

This research work was supported by the UK EPSRC and our industrial partners in the Next Generation Inkjet Printing Consortium, and is published with permission. We would also like to thank Dr Tri Tuladhar of the University of Cambridge, Department of Chemical Engineering, for preparation and characterization of the dilute polymer samples and Dr Mark Crankshaw of Xaar plc, Cambridge, for helpful discussions on the operation of the XJ126-200 print head, software and interfaces.

References

1. I.M. Hutchings, G.D. Martin, and S.D. Hoath, "High Speed Imaging and Analysis of Jet and Drop Formation", J. Imaging Sci. and Technol., in press (2007).
2. G.D. Martin, et al., Jet formation and late-stage ligament instability in drop-on-demand printing, Proc. NIP22, pg. 95 (2006).
3. H.M. Dong, W.W. Carr, and J.F. Morris, "An experimental study of drop-on-demand drop formation", Physics of Fluids, 18, 072102 (2006).
4. J. de Jong, et al., "Entrapped air bubbles in piezo-driven inkjet printing: Their effect on the droplet velocity", Physics of Fluids, 18, 121511 (2006).
5. H.J. Shore and G.M. Harrison, "The effect of added polymers on the formation of drops ejected from a nozzle", Physics of Fluids, 17, 033104 (2005).
6. X.D. Shi, M.P. Brenner, and S.R. Nagel, "A Cascade of Structure in a Drop Falling from a Faucet", Science, 265, 219 (1994).
7. S.T. Thoroddsen and K. Takehara, "The coalescence cascade of a drop", Physics of Fluids, 12, 1265 (2000).
8. M. Abramowitz and I.A. Stegun, Handbook of Mathematical Functions, (Dover Publications Inc., New York, 1972) pg. 930.
9. E. Villermaux, P. Marmottant, and J. Duplat, "Ligament-mediated spray formation", Physical Review Letters, 92, 074501 (2004).

Author biography

Stephen Hoath received his B.A. in physics (1972) and his D.Phil. in nuclear physics from the University of Oxford (1977). He has since taught and worked in research and development in academia and industry. His research work has recently focused on the fundamentals of inkjet printing at the Inkjet Research Centre at the University of Cambridge, UK. He is a member of AVS, IOP and is a Chartered Physicist, Engineer and Scientist.